J. Math. Biol. (2013) 66:1463–1474
DOI 10.1007/s00285-012-0540-y

Mathematical Biology

Epidemic models with uncertainty in the reproduction number

M. G. Roberts

Received: 8 August 2011 / Revised: 15 April 2012 / Published online: 5 May 2012

Abstract One of the first quantities to be estimated at the start of an epidemic is the basic reproduction number, $\mathcal{R}_0$. The progress of an epidemic is sensitive to the value of $\mathcal{R}_0$, hence we need methods for exploring the consequences of uncertainty in the estimate. We begin with an analysis of the *SIR* model, with $\mathcal{R}_0$ specified by a probability distribution instead of a single value. We derive probability distributions for the prevalence and incidence of infection during the initial exponential phase, the peaks in prevalence and incidence and their timing, and the final size of the epidemic. Then, by expanding the state variables in orthogonal polynomials in uncertainty space, we construct a set of deterministic equations for the distribution of the solution throughout the time-course of the epidemic. The resulting dynamical system need only be solved once to produce a *deterministic stochastic* solution. The method is illustrated with $\mathcal{R}_0$ specified by uniform, beta and normal distributions. We then apply the method to data from the New Zealand epidemic of H1N1 influenza in 2009. We apply the polynomial expansion method to a Kermack–McKendrick model, to simulate a forecasting system that could be used in real time. The results demonstrate the level of uncertainty when making parameter estimates and projections based on a limited amount of data, as would be the case during the initial stages of an epidemic. In solving both problems we demonstrate how the dynamical system is derived automatically via recurrence relationships, then solved numerically.

Funded by Health Research Council Grant HRC 10/754.

M. G. Roberts (✉)
Infectious Disease Research Centre, Institute of Information and Mathematical Sciences,
New Zealand Institute for Advanced Study, Massey University, Private Bag 102 904,
North Shore Mail Centre, Auckland, New Zealand
e-mail: m.g.roberts@massey.ac.nz

Keywords *SIR* model · Kermack–McKendrick model · Basic reproduction number · Uncertainty

Mathematics Subject Classification 92D30

1 Introduction

The basic reproduction number, $\mathcal{R}_0$, is probably the most important quantity in epidemiology (Diekmann and Heesterbeek 2000; Roberts 2007), and during the emergence of a new infectious disease it is one of the first quantities to be estimated. Some estimation schemes are essentially deterministic (Roberts and Heesterbeek 2007; Wallinga and Lipsitch 2007), deriving a value of $\mathcal{R}_0$ from the rate of exponential increase at the beginning of the epidemic. Others also provide a measure of the uncertainty around the estimate, see for example Roberts and Nishiura (2011) and the references cited therein. Given an estimate of $\mathcal{R}_0$ we can project the future course of the epidemic. Here we present a method for doing that, while taking the uncertainty of the estimate into account.

To illustrate the concept and method, we first consider a simple problem: the *SIR* epidemic model (Diekmann and Heesterbeek 2000; Roberts 2007) of the form:

$$\begin{aligned} \dot{x}(t) &= -(\mathcal{R}_0 + \rho\theta)\, xy \\ \dot{y}(t) &= (\mathcal{R}_0 + \rho\theta)\, xy - y \end{aligned} \tag{1}$$

with initial conditions $x(0) = x_0$ and $y(0) = y_0 \ll 1$; where $x(t)$ is the proportion of the population susceptible at time t, and $y(t)$ is the proportion of the population infectious. Time has been scaled so that the mean generation interval is one. The basic reproduction number, $\mathcal{R}_0$, is assumed to be subject to some uncertainty, represented by the random variable θ, and $\rho > 0$ is a scaling parameter. We derive expressions for the prevalence of infection during the initial exponential growth phase, the peaks in prevalence and incidence and their timing, and the final size of the epidemic. These are presented as probability density functions (PDFs), depending on the underlying distribution of the random variable θ. We focus on the situations where θ is either uniformly or beta distributed on the interval $[-1, 1]$. We also present the results obtained when θ is normally distributed for comparison. We then take the model described by Eq. (1) and expand the state variables as truncated series of orthogonal polynomials in θ, then numerically solve the problem for a complete epidemic.

As a more applied example, we derive a discrete-time version of the Kermack–McKendrick model (Diekmann and Heesterbeek 2000) with local and imported cases. We use this to make a retrospective projection of the initial part of the epidemic curve for influenza H1N1 in New Zealand, that could have been made on June 22 2009, using the reported incidence of infection up to that date. In doing this we adopt the gamma distribution estimated for the mean generation interval from overseas data (Fraser et al. 2009). Hence we are using information that would have been available at that stage in the epidemic. This illustrates the potential application of the model as a means of real-time forecasting.

1.1 Properties of the *SIR* model

If $\rho = 0$ we have the well-known results for a deterministic model (see Diekmann and Heesterbeek 2000; Roberts 2007): an epidemic occurs if $\mathcal{R}_0 x_0 > 1$; the proportion of the population that is infected may be approximated initially by $y(t) = y_0 e^{\mathcal{R}_0 x_0 t - t}$; during the epidemic $y + C(x)$ is a conserved quantity, where $C(x) = x - \mathcal{R}_0^{-1} \log x$; and the proportion of the population that is infected during the epidemic, $P = x_0 - x_\infty$, solves the final size equation

$$\mathcal{R}_0 + \frac{1}{P} \log\left(1 - \frac{P}{x_0}\right) = 0 \tag{2}$$

Peak prevalence occurs when $t = t_{\text{pp}}$, where $x_{\text{pp}} = \mathcal{R}_0^{-1}$ and $y_{\text{pp}} = y_0 + C(x_0) - C(x_{\text{pp}})$. Hence

$$t_{\text{pp}} = \int_{x_{\text{pp}}}^{x_0} \frac{\mathrm{d}x}{\mathcal{R}_0 x \, (y_0 + C(x_0) - C(x))} \tag{3}$$

The incidence of infection, $\iota(t) = \mathcal{R}_0 x(t) y(t)$, solves

$$\frac{\mathrm{d}\iota}{\mathrm{d}t} = \iota \, (\mathcal{R}_0 x - \mathcal{R}_0 y - 1)$$

Peak incidence occurs when $x_{\text{pi}} = y_{\text{pi}} + \mathcal{R}_0^{-1} = x(t_{\text{pi}})$. As $x(t)$ is a decreasing function of time, $t_{\text{pi}} < t_{\text{pp}}$. The value of x_{pi} may be found by solving $x_{\text{pi}} + C(x_{\text{pi}}) = \mathcal{R}_0^{-1} + y_0 + C(x_0)$. The time to peak incidence may be found from a similar equation to (3), simply replace the lower limit of integration with x_{pi}. In the next section, we investigate the changes in these results, and in the dynamics of the system, when θ is chosen from a probability distribution with mean zero.

2 The effect of uncertainty in $\mathcal{R}_0$

We emphasize the dependence of solutions of Eq. (1) on the random variable θ, by writing the dependent variables $x(t, \theta)$ and $y(t, \theta)$. We refer to $x(t, 0)$, $y(t, 0)$ as the deterministic solution, as it is the solution obtained when $\mathcal{R}_0$ is set to the mean estimated value.

2.1 Exponential growth

The solution for the proportion infectious during the initial exponential phase is $y(t, \theta) = y_0 e^{(\mathcal{R}_0 + \rho\theta) x_0 t - t}$. If θ is chosen from a distribution with PDF $w(\theta)$, then the expected value of $y(t, \theta)$ is

$$\mathbb{E}(y) = \int_{\Omega} y(t,\theta)w(\theta)\,\mathrm{d}\theta = y_0 e^{\mathcal{R}_0 x_0 t - t} W(t)$$

where Ω is the support of w. The function $W(t) = \int_\Omega e^{\rho\theta x_0 t} w(\theta)\,\mathrm{d}\theta$ is a correction factor that multiplies the deterministic solution. As the exponential function is concave, if $\mathbb{E}(\theta) = 0$ then $W(t) > 1$ for $t > 0$ by Jensen's inequality (Grimmett and Stirzaker 1992).

Example 1 If θ is uniformly distributed on $\Omega = [-1, 1]$, then $w(\theta) = \frac{1}{2}$ and $W(t) = \frac{\sinh \rho x_0 t}{\rho x_0 t}$.

Example 2 If θ has a standard normal distribution, then $w(\theta) = \frac{1}{\sqrt{2\pi}} e^{-\theta^2/2}$, $\Omega = \mathbb{R}$, and $W(t) = e^{(\rho x_0 t)^2/2}$. Note that for this example $\mathcal{R}_0 + \rho\theta$ is less than one, or even less than zero, for some values of θ. This problem may be overcome by approximating the normal distribution with a beta distribution over a finite interval.

Example 3 If θ has a symmetric beta distribution, then $w(\theta) = k(1-\theta^2)^\beta$, $\Omega = [-1, 1]$, and k is a normalising constant (see Appendix). The correction factor $W(t) = e^{-\rho x_0 t}\, {}_1F_1(\beta+1; 2\beta+2; 2\rho x_0 t)$, where ${}_1F_1$ is the confluent hypergeometric function of the first kind (see Abramowitz and Stegun 1970, Chapter 13).

Results similar to the first two examples may be found in Xiu and Karniadakis (2002). For Example 3, note that $\lim_{\rho\to 0} {}_1F_1(\beta+1; 2\beta+2; 2\rho x_0 t) = 1$; and that for large β, $w(\theta) \to \delta(\theta)$, and $\lim_{\beta\to\infty} {}_1F_1(\beta+1; 2\beta+2; 2\rho x_0 t) = e^{\rho x_0 t}$. Hence the deterministic solution is reached both in the limit of the distribution and as the parameter ρ tends to zero. When the normal and beta distributions are compared, the beta distribution with $\beta = 1.19$ is seen to approximate the normal distribution with $\sigma = \frac{1}{2}$ on $(-1, 1)$.

As y is an increasing function of θ, the PDF for y at time t is $f(y) = \frac{w(\theta(y))}{\rho x_0 t y}$, where $\theta(y)$ is the solution of $y = y_0 e^{(\mathcal{R}_0+\rho\theta)x_0 t - t}$. The function $f(y)$, with $w(\theta)$ specified by each of the example distributions is shown in Fig. 1a.

2.2 The epidemic peaks

For a fixed θ, the quantity $y(t,\theta) + C(x(t,\theta),\theta)$ is conserved over t, where

$$C(x(t,\theta),\theta) = x(t,\theta) - \frac{\log x(t,\theta)}{\mathcal{R}_0 + \rho\theta}$$

At peak prevalence $x_{\mathrm{pp}}(\theta) = (\mathcal{R}_0 + \rho\theta)^{-1}$ and $y_{\mathrm{pp}}(\theta) = y_0 + C(x_0,\theta) - C(x_{\mathrm{pp}}(\theta),\theta)$. The PDFs of x_{pp} and y_{pp}, with $w(\theta)$ specified by each of the example distributions are shown in Fig. 1b. Also shown are the distribution means, $\mathbb{E}(x_{\mathrm{pp}})$ and $\mathbb{E}(y_{\mathrm{pp}})$, calculated numerically, and the deterministic peak values obtained when $\theta = 0$. Note that $x_{\mathrm{pp}}(\theta)$ and $y_{\mathrm{pp}}(\theta)$ are peak values, which occur at different times depending on the value of θ. Hence their distributions do not necessarily correspond to the distributions of x or y at any value of t. Adding uncertainty to Eq. (3) we obtain

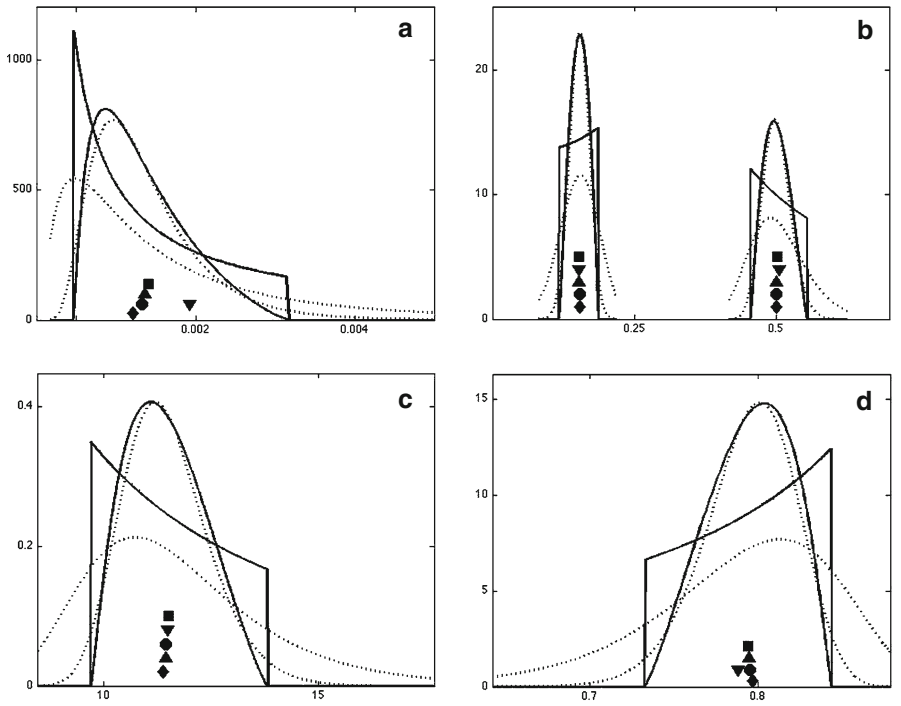

Fig. 1 **a** Probability density functions (PDFs) for $y(t,\theta)$ at $t = 4.8$; **b** PDFs for $x_{\rm pp}(\theta)$ (*right*) and $y_{\rm pp}(\theta)$ (*left*); **c** PDFs for $t_{\rm pp}(\theta)$; and **d** PDFs for $P(\theta)$; with $w(\theta)$ a uniform distribution (*vertical sides*) or a beta distribution ($\beta = 1.19$). Also shown dotted are results with θ normally distributed ($\sigma = 1$ and $\sigma = 0.5$). The *solid markers* are at the expected values of the distributions: uniform (*square*); beta (*circle*); normal $\sigma = 0.5$ (*triangle pointing up*); normal $\sigma = 1$ (*triangle pointing down*); and the deterministic solution ($\theta = 0$ *diamond*). The vertical displacement of the marker is only for clarity of display, and has no numerical significance. Parameter values are $\mathcal{R}_0 = 2$, $\rho = 0.2$, $x_0 = 1 - y_0$, $y_0 = 10^{-5}$

$$t_{\rm pp}(\theta) = \int_{(\mathcal{R}_0+\rho\theta)^{-1}}^{x_0} \frac{{\rm d}x}{((\mathcal{R}_0+\rho\theta)\,(x_0+y_0-x)+\log\,(x/x_0))\,x}$$

The PDFs of $t_{\rm pp}$ are shown in Fig. 1c.

At peak incidence $y_{\rm pi}(\theta) = x_{\rm pi}(\theta) - (\mathcal{R}_0+\rho\theta)^{-1} = C(x_0,\theta) - C(x_{\rm pi}(\theta),\theta)$. For fixed θ, x is a decreasing function of t, hence $x_{\rm pi}(\theta) > x_{\rm pp}(\theta)$ and incidence always peaks before prevalence. The PDFs of $x_{\rm pi}$, $t_{\rm pi}$ and $t_{\rm pi}$ may be calculated numerically, and presented in a similar manner to those at peak prevalence (results not shown).

2.3 The final size

Adding uncertainty to the final size equation, Eq. (2),

$$\mathcal{R}_0 + \rho\theta + \frac{1}{P(\theta)}\log\left(1 - \frac{P(\theta)}{x_0}\right) = 0$$

The PDF of P, with $w(\theta)$ following each of the example distributions is shown in Fig. 1d. Also shown are the distribution means, $\mathbb{E}(P)$, calculated numerically, and the deterministic final size from Eq. (2).

2.4 The numerical solution

We now construct an approximate solution to Eq. (1) using a Galerkin method. Let $\{\phi_i(\theta)\}$ represent a basis for functions defined on Ω. Substitute $x(t,\theta) = \sum_{i=1}^{\infty} x_i(t)\phi_i(\theta)$ and $y(t,\theta) = \sum_{i=1}^{\infty} y_i(t)\phi_i(\theta)$ in Eq. (1) to obtain

$$\sum_{i=1}^{\infty} \dot{x}_i(t)\phi_i(\theta) = -(\mathcal{R}_0 + \rho\theta) \sum_{i=1}^{\infty}\sum_{j=1}^{\infty} x_i(t)y_j(t)\phi_i(\theta)\phi_j(\theta)$$

$$\sum_{i=1}^{\infty} \dot{y}_i(t)\phi_i(\theta) = (\mathcal{R}_0 + \rho\theta) \sum_{i=1}^{\infty}\sum_{j=1}^{\infty} x_i(t)y_j(t)\phi_i(\theta)\phi_j(\theta) - \sum_{i=1}^{\infty} y_i(t)\phi_i(\theta)$$

We define an inner product by $\mathbb{E}(\phi_i\phi_j) = \int_\Omega \phi_i(\theta)\phi_j(\theta)w(\theta)\,\mathrm{d}\theta$. Hence we choose our polynomial basis so that $\mathbb{E}(\phi_i\phi_j) = 0$ if $i \neq j$, and the choice of polynomial depends on the distribution of θ. If we truncate the sequence of polynomials at $i = n$, we have $2n$ differential equations to solve:

$$\begin{aligned} \dot{x}_\ell(t) &= -\mathbf{x}.\left(\mathcal{R}_0\mathbf{A}_\ell + \rho\mathbf{B}_\ell\right)\mathbf{y} \\ \dot{y}_\ell(t) &= \mathbf{x}.\left(\mathcal{R}_0\mathbf{A}_\ell + \rho\mathbf{B}_\ell\right)\mathbf{y} - y_\ell \end{aligned} \tag{4}$$

for $\ell = 1,\ldots,n$ with $\mathbf{x} = (x_1, x_2, \ldots, x_n)'$, similarly $\mathbf{y}$ (prime is transpose). The $n \times n$ matrices $\mathbf{A}_\ell$ and $\mathbf{B}_\ell$ have components

$$A_{\ell i j} = \frac{\mathbb{E}\left(\phi_i\phi_j\phi_\ell\right)}{\mathbb{E}\left(\phi_\ell^2\right)} \qquad B_{\ell i j} = \frac{\mathbb{E}\left(\theta\phi_i\phi_j\phi_\ell\right)}{\mathbb{E}\left(\phi_\ell^2\right)}$$

respectively. The initial conditions are $\mathbf{x}(0) = x_0\mathbf{e}$ and $\mathbf{y}(0) = y_0\mathbf{e}$, where $\mathbf{e}$ is a unit vector with $e_i = 0$ for $i > 1$.

Two examples of the numerical solution of Eq. (4) are shown in Fig. 2. For Fig. 2a, b, θ is uniformly distributed on $[-1, 1]$, and the $\phi_i(\theta)$ are Legendre polynomials. For Fig. 2c, d, θ has a beta distribution on $[-1, 1]$, and the $\phi_i(\theta)$ are Jacobi polynomials. See the Appendix for more details. Comparing Fig. 2a, b and c, d, we see that the limits of the solutions and the deterministic solutions ($\rho = 0$) are identical, but the eigenfunctions and expected values are different. As would be expected, the quartiles either side of the mean are narrower when θ has a beta distribution (Fig. 2c, d) than when θ has a uniform distribution (Fig. 2a, b). If we took θ to be normally distributed, we would take $\phi_i(\theta)$ to be Hermite polynomials (Xiu 2010). However, this led to convergence problems, because Hermite polynomials are defined over the real line, and regions of the parameter space then correspond to different qualitative dynamics. For the solutions illustrated we have $\mathcal{R}_0 + \rho\theta > 1$ for all θ.

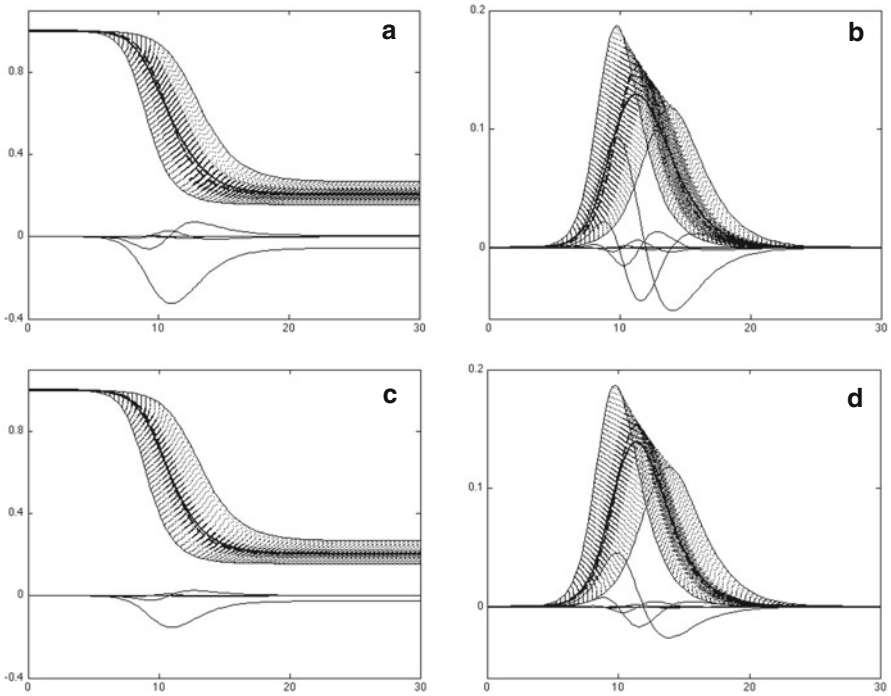

Fig. 2 **a**, **b** Numerical solution of the *SIR* model with θ obeying a uniform distribution. **a** Time series for x; **b** time series for y; **c, d** numerical solution of the model with θ obeying a symmetric beta distribution. **c** Time series for x; **d** time series for y. *Solid lines* are expected values at time t, *dashed lines* are deterministic solutions, $\theta = 0$, dense points are values in the inner quartiles, $|\theta| < \frac{1}{2}$, less dense points are values in the outer quartiles, $\frac{1}{2} < |\theta| < 1$. *Thin lines* show the eigenfunctions $x_i(t)$ (**a, c**) and $y_i(t)$ (**b, d**), diminishing in magnitude with increasing i. Parameter values are $\mathcal{R}_0 = 2$, $\rho = 0.2$, $x_0 = 1 - 10^{-5}$, $y_0 = 10^{-5}$

3 Uncertainty in the Kermack–McKendrick model

In the continuous time domain, the incidence of an invading infection causing an epidemic in a population of size N is given by Diekmann and Heesterbeek (2000), Roberts and Nishiura (2011)

$$\iota(t) = \mathcal{R}x(t)\,(f * \iota + g * \jmath) \tag{5}$$

where $\mathcal{R}$ is the effective reproduction number at the beginning of the epidemic, $f(\tau)$ is the probability distribution of infection-generation intervals, $\jmath(t)$ is the incidence of imported cases and $g(\tau)$ is a modification of $f(\tau)$ to account for delays in transit. Hence $\iota(t)$ refers only to locally transmitted cases. The convolution is defined by $f * \iota = \int_0^\infty f(\tau)\iota(t-\tau)\,\mathrm{d}\tau$. The proportion of the population that is susceptible at time t is

$$x(t) = x_0 - \frac{1}{N}\int_0^t \iota(u)\,\mathrm{d}u \tag{6}$$

and we assume that N is constant. For an invading infectious disease, we cannot necessarily assume that the population is susceptible at $t = 0$, hence the use of $\mathcal{R}$ instead of $\mathcal{R}_0$. Also, data are often collected in daily incidence values, so a discrete-time model is more compatible with observations. The equivalent model to Eqs. (5, 6) is

$$I_t = \mathcal{R} X_t \left(F * I_t + G * J_t\right) \tag{7}$$

where I_t and J_t are the daily incidences of locally-transmitted and imported cases respectively, $F * I_t = \sum_{s=1}^{m} F_s I_{t-s}$ (similarly $G * J_t$), and $X_t = X_0 - \frac{1}{N}\sum_{s=1}^{t-1} I_s$.

3.1 The numerical solution

We now analyse the discrete-time model (7) using the methodology described in Sect. 2.4. Assume the estimated effective reproduction number at the beginning of the epidemic to be $\mathcal{R} + \rho\theta$, where θ is a random variable with mean zero. Let $I_t(\theta) = \sum_{i=1}^{\infty} I_{ti}\phi_i(\theta)$ and $X_t(\theta) = \sum_{i=1}^{\infty} X_{ti}\phi_i(\theta)$. Then Eq. (7) becomes

$$\sum_{i=1}^{\infty} I_{ti}\phi_i(\theta) = (\mathcal{R} + \rho\theta)\sum_{i=1}^{\infty} X_{ti}\phi_i(\theta)\left(\left(\sum_{j=1}^{\infty} F * I_{tj}\phi_j(\theta)\right) + G * J_t\right)$$

Multiplying by $\phi_\ell(\theta)w(\theta)$ and integrating over Ω, we obtain

$$\begin{aligned} I_{t\ell} = \sum_{i=1}^{\infty}\sum_{j=1}^{\infty} X_{ti}\left(\mathcal{R}\frac{\mathbb{E}\left(\phi_i\phi_j\phi_\ell\right)}{\mathbb{E}\left(\phi_\ell^2\right)} + \rho\frac{\mathbb{E}\left(\theta\phi_i\phi_j\phi_\ell\right)}{\mathbb{E}\left(\phi_\ell^2\right)}\right)F * I_{tj} \\ + \left(\mathcal{R}X_{t\ell} + \rho\sum_{i=1}^{\infty}\frac{\mathbb{E}\left(\theta\phi_i\phi_\ell\right)}{\mathbb{E}\left(\phi_\ell^2\right)}X_{ti}\right)G * J_t \end{aligned}$$

Define row vectors $\mathbf{I}_t$ and $\mathbf{X}_t$, such that the i^{th} entry is equal to I_{ti} or X_{ti} respectively. Then, after truncation

$$I_{t\ell} = \mathbf{X}_t\left(\mathcal{R}\mathbf{A}_\ell + \rho\mathbf{B}_\ell\right)\left(F * \mathbf{I}_t\right)' + \left(\mathcal{R}X_{t\ell} + \rho\mathbf{X}_t\mathbf{c}_\ell\right)G * J_t \tag{8}$$

The matrices $\mathbf{A}_\ell$ and $\mathbf{B}_\ell$ are as defined in Sect. 2.4, the vector $\mathbf{c}_\ell$ has components $c_{\ell i} = \mathbb{E}(\theta\phi_i\phi_\ell)/\mathbb{E}(\phi_\ell^2)$, and $\mathbf{X}_t = \mathbf{X}_0 - \frac{1}{N}\sum_{s=1}^{t-1}\mathbf{I}_s$.

3.2 Example: influenza H1N1-2009 in New Zealand

During the 2009 epidemic of pandemic strain influenza A H1N1 in New Zealand, cases were tested and confirmed up to June 22. The daily incidence data from May 19 to June 30 are shown in Fig. 3, subdivided into cases with a relevant history of overseas travel, and cases that were presumed to arise from local transmission. The data to June 21 (shown with a vertical line) were used to estimate $\mathcal{R} = 1.25$,

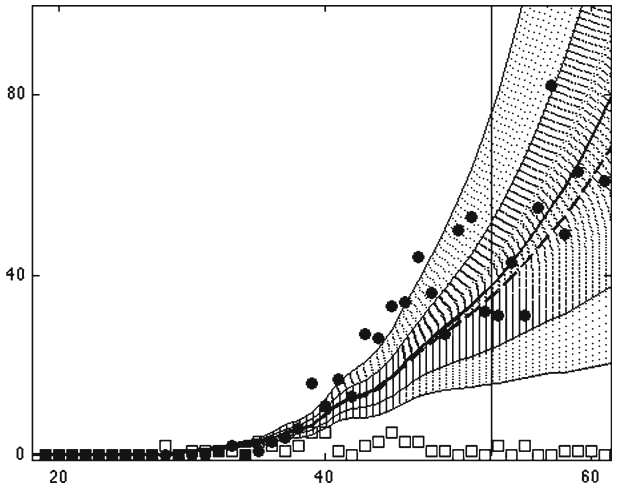

Fig. 3 Influenza H1N1-2009 in New Zealand. Data points are daily incidence of imported cases (*white squares*) and locally-transmitted cases (*black circles*). The *horizontal axis* is days, day one is 1 May 2009. Data up to day 52 (June 21, *vertical line*) were used to estimate $\mathcal{R}$. The projection is shown as an expected value, with the range ($1.05 < \mathcal{R} < 1.45$) *shaded* and the inner quartiles ($1.15 < \mathcal{R} < 1.35$) more *densely shaded*. The deterministic solution for $\mathcal{R} = 1.25$ is shown *dashed*

with confidence intervals (1.07, 1.47) (Roberts and Nishiura 2011). If we had made this estimate on June 22, and approximated the uncertainty around the estimate with $\rho = 0.2$ and θ beta-distributed with $\beta = 1.19$, then we could have made the projection of future incidence presented in Fig. 3. In compiling Fig. 3 we assumed $F = G = (0.0300, 0.2397, 0.3307, 0.2321, 0.1328)$ in line with the gamma distribution estimated for H1N1 early in the 2009 epidemic (Fraser et al. 2009), see also Roberts and Nishiura (2011). The continued projection after June 22 is made on the basis of no further imported cases, and if used in real time would be updated as further data were obtained. The incidence of locally-transmitted and imported cases to the end of June is shown for comparison.

4 Discussion

We have presented a method for incorporating uncertainty in the estimate of the basic reproduction number in a deterministic model of an epidemic. Starting with the well-known *SIR* model we can derive explicit solutions for the prevalence in the initial growth phase, the timing and magnitude of the epidemic peaks, and the final size of the epidemic. One interesting result is that the deterministic solution for the prevalence of infection during the growth phase is always less than the 'expected solution'. This can be seen in Figs. 1a, 2b, d, and 3. Hence, using the mean of the $\mathcal{R}_0$ estimate in a deterministic model results in a biased projection of the epidemic. Another interesting result is that the peak in infection incidence always occurs before the peak in prevalence, hence one should not refer to an infection peak without specifying which. However, health authorities frequently want to know about the timing and magnitude

of the peak or peaks, and our method provides a probability distribution for these estimates.

The numerical solution presented in Sect. 2.4 provides a clear advantage over repeated numerical solution of the deterministic equations, with $\mathcal{R}_0$ sampled *a priori* from a distribution. It is true that if one only wanted the solution at the quartiles, then just five numerical solutions of Eq. (1) would suffice. However, to find the expected solution or other moments as functions of t, or the PDF at particular values of t, then many more evaluations would be required. In contrast, although we have replaced two equations with $2n$ equations, we only need to solve these once. The matrices $\mathbf{A}_\ell$ and $\mathbf{B}_\ell$ are first evaluated numerically using the appropriate recurrence relationships for the orthogonal polynomials. The resulting set of ordinary differential equations is then solved, the entire operation requiring only a simple routine and the appropriate numerical software. The results presented here were obtained using Matlab 2010a (The MathWorks, Inc.). The choice of the uniform and beta distributions for our illustrations was to demonstrate two aspects. First, if only a range of $\mathcal{R}_0$ is known, then the uniform distribution is appropriate. Second, if the estimate is obtained with a likelihood profile assumed to be normal, then this may be approximated by the beta distribution. If we had taken θ to be normally distributed, then it would have been appropriate to use Hermite polynomials for the functions ϕ (Xiu 2010; Xiu and Karniadakis 2002). As these do not have compact support, then $\mathcal{R}_0 + \rho\theta$ can take values less than one, or even less than zero. Including these values where different qualitative behaviour occurs in the numerical solutions led to instabilities. Approximating the normal distribution with the beta distribution over a finite interval overcame this problem.

The solution presented in Sect. 2.4 shows an epidemic running to its conclusion, which would be unlikely as control measures or even the reaction of the public would change its dynamics. However, such calculations are frequently presented as baseline projections, so that the potential effects of different control interventions may be assessed (Ferguson et al. 2005, 2006; Germann et al. 2006; Longini et al. 2005; Roberts et al. 2007; Wu et al. 2006). It is also based on the *SIR* model, being the simplest but also most widely used mathematical representation of an epidemic. The retrospective projection of the influenza A H1N1 epidemic in New Zealand in 2009 illustrates the potential for this methodology to be used as a real-time forecasting system in future epidemics. One such system was developed for Singapore (Ong et al. 2010). Tools such as these are in demand by health authorities, and we intend to apply this methodology to the next pandemic of an emerging infectious disease.

Although the models discussed in this paper address uncertainty in the estimation of the basic reproduction number, they are deterministic in nature. The variability of solutions illustrated in Figs. 1, 2 and 3 could have been achieved by generating a large number of solutions of Eq. (1) with different parameter values, chosen from a prescribed distribution. Instead we have used an orthogonal expansion to derive a larger set of differential equations, which we then solved once. Solutions of a stochastic version of the model would show variability due to different realisations of the model having a different outcome. The differences are usually due to individuals in the model having contact with other individuals randomly in time, according to some stochastic process. For an overview of stochastic epidemic models see Britton (2010). Note in particular the qualitative similarity between the shapes of the final size distribution in

Fig. 1d, and the final size distribution of a major epidemic in Fig. 3 of Britton (2010). However, with a stochastic model a minor outbreak (where the epidemic fails to 'take off') is also a possible outcome, even when $\mathcal{R}_0 > 1$ (Britton 2010; Diekmann and Heesterbeek 2000), whereas for the method presented here all epidemics are deterministic with $\mathcal{R}_0 > 1$, and hence major outbreaks.

Acknowledgments The author would like to thank Carlo Laing for pointing out the book by Xiu (2010), and two anonymous referees whose suggestions led to improvements in the manuscript.

Appendix

Legendre polynomials If θ is uniformly distributed on $[-1, 1]$ then $\phi_i(\theta) = P_{i-1}(\theta)$, the Legendre polynomial, and $w(\theta) = \frac{1}{2}$. The first two polynomials are $P_0(\theta) = 1$ and $P_1(\theta) = \theta$; all subsequent polynomials may be found from the recurrence relationship

$$P_{\ell+1}(\theta) = \frac{2\ell+1}{\ell+1}\theta P_\ell(\theta) - \frac{\ell}{\ell+1}P_{\ell-1}(\theta)$$

The orthogonality relationship is

$$\mathbb{E}\left(\phi_i\phi_j\right) = \mathbb{E}\left(P_{i-1}P_{j-1}\right) = \frac{\delta_{ij}}{2j-1}$$

with $\delta_{ii} = 1$, $\delta_{ij} = 0$ if $i \neq j$, and we have the integral identity $\mathbb{E}\left(\theta^n\right) = \frac{1}{n+1}$ if n even, and zero if n odd.

Jacobi polynomials If θ has a symmetric beta distribution on $[-1, 1]$ then $\phi_i(\theta) = J_{i-1}^{(\beta)}(\theta)$, the symmetric Jacobi polynomial, and $w(\theta) = k(1-\theta^2)^\beta$, where

$$\frac{1}{k} = \int_{-1}^{1}(1-\theta^2)^\beta \,\mathrm{d}\theta = \frac{2^{2\beta+1}\Gamma(\beta+1)^2}{\Gamma(2\beta+2)}$$

In Xiu (2010) the Jacobi polynomials are written $P_n^{(\alpha,\beta)}(x)$. We are interested in symmetric distributions, so $J_\ell^{(\beta)}(\theta) = P_\ell^{(\beta,\beta)}(\theta)$. The first two polynomials are $J_0^{(\beta)}(\theta) = 1$ and $J_1^{(\beta)}(\theta) = (\beta+1)\,\theta$. All subsequent polynomials may be found from the recurrence relationship

$$J_{\ell+1}^{(\beta)}(\theta) = \frac{(2\ell+2\beta+1)\,(\ell+\beta+1)}{(\ell+1)\,(\ell+2\beta+1)}\theta J_\ell^{(\beta)}(\theta) - \frac{(\ell+\beta)\,(\ell+\beta+1)}{(\ell+1)\,(\ell+2\beta+1)}J_{\ell-1}^{(\beta)}(\theta)$$

The orthogonality relationship is

$$\mathbb{E}\left(\phi_i\phi_j\right) = \mathbb{E}\left(J_{i-1}^{(\beta)}J_{j-1}^{(\beta)}\right) = \frac{\Gamma(j+\beta+1)^2\Gamma(2\beta+2)\delta_{ij}}{j!\,(2j+2\beta+1)\,\Gamma(j+2\beta+1)\Gamma(\beta+1)^2}$$

and $\mathbb{E}\left(\theta^{n+2}\right) = \frac{n+1}{n+2\beta+3}\mathbb{E}\left(\theta^n\right)$ if n even, and zero if n odd.

References

Abramowitz M, Stegun IA (1970) Handbook of mathematical functions. Dover, New York
Britton T (2010) Stochastic epidemic models: a survey. Math Biosci 225:24–35
Diekmann O, Heesterbeek JAP (2000) Mathematical epidemiology of infectious diseases: model building, analysis and interpretation. Wiley, Chichester
Ferguson N, Cummings DAT, Cauchemez S, Fraser C, Riley S, Meeyai A, Iamsirithaworn S, Burke DS (2005) Strategies for containing an emerging influenza pandemic in Southeast Asia. Nature 437:209–214
Ferguson N, Cummings DAT, Fraser C, Cajka JC, Cooley PC, Burke DS (2006) Strategies for mitigating an influenza pandemic. Nature 442:448–452
Fraser C, Donnelly CA, Cauchemez S, Hanage WP, Van Kerkhove MD, Hollingsworth TD, Griffin J, Baggaley RF, Jenkins HE, Lyons EJ, Jombart T, Hinsley WR, Grassly NC, Balloux F, Ghani AC, Ferguson NM, Rambaut A, Pybus OG, Lopez-Gatell H, Apluche-Aranda CM, Chapela IB, Zavala EP, Guevara DM, Checchi F, Garcia E, Hugonnet S, Roth C (2009) The WHO Rapid Pandemic Assessment Collaboration. Pandemic potential of a strain of influenza A (H1N1): early findings. Science 324:1557–1561
Germann TC, Kadau K, Longini IM, Macken CA (2006) Mitigation strategies for pandemic influenza in the United States. PNAS 103:5935–5940
Grimmett GS, Stirzaker DR (1992) Probability and random processes, 2nd edn. Oxford University Press, Oxford
Longini IM, Nizam A, Xu S, Ungchusak K, Hanshaoworakul W, Cummings DAT, Halloran ME (2005) Containing pandemic influenza at the source. Science 309:1083–1087
Ong JBS, Chen M-C, Cook AR, Lee HC, Lee VJ, Lin RTP, Tambyah PA, Goh LG (2010) Real-time epidemic monitoring and forecasting of H1N1-2009 using influenza-like illness from general practice and family doctor clinics in Singapore. PLoS One 5:e10036
Roberts MG, Baker M, Jennings LC, Sertsou G, Wilson N (2007) A model for the spread and control of pandemic influenza in an isolated geographical region. J R Soc Interface 4:325–330
Roberts MG (2007) The pluses and minuses of $\mathcal{R}_0$. J R Soc Interface 4:949–961
Roberts MG, Heesterbeek JAP (2007) Model-consistent estimation of the basic reproduction number from the incidence of an emerging infection. J Math Biol 55:803–816
Roberts MG, Nishiura H (2011) Early estimation of the reproduction number in the presence of imported cases: pandemic influenza H1N1-2009 in New Zealand. PLoS One 6:e17835
Wallinga J, Lipsitch M (2007) How generation intervals shape the relationship between growth rates and reproductive numbers. Proc R Soc Ser B 274:599–604
Wu JT, Riley S, Fraser C, Leung GM (2006) Reducing the impact of the next influenza pandemic using household-based public health interventions. PLoS Med 3:1532–1540
Xiu D (2010) 2010 Numerical methods for stochastic computations. Princeton University Press, Princeton
Xiu D, Karniadakis G (2002) The Wiener–Askey polynomial chaos for stochastic differential equations. SIAM J Sci Comput 24:619–644